
Neural Complexity Measures

Yoonho Lee¹, Juho Lee^{1,2}, Sung Ju Hwang^{1,2}, Eunho Yang^{1,2}, Seungjin Choi³
 AITRICS¹, Seoul, South Korea, KAIST², Daejeon, South Korea, BARO AI³, Seoul, South Korea
 eddy@aitrics.com

Abstract

While various complexity measures for diverse model classes have been proposed, specifying an appropriate measure capable of predicting and explaining generalization in deep networks has proven to be challenging. We propose *Neural Complexity* (NC), an alternative data-driven approach that meta-learns a scalar complexity measure through interactions with a large number of heterogeneous tasks. The trained NC model can be added to the standard training loss to regularize any task learner under standard learning frameworks. We contrast NC’s approach against existing manually-designed complexity measures and also against other meta-learning models, and validate NC’s performance on multiple regression and classification tasks.

1 Introduction

Deep neural networks have achieved excellent performance on numerous tasks, including image classification [Krizhevsky et al., 2012] and board games [Silver et al., 2017]. Although they achieve superior empirical performance, why and how these models generalize remains a mystery. Thus, understanding what properties of deep networks allows them to generalize is an important problem with far-reaching potential benefits such as principled model design and safety-aware models. To explain why deep networks generalize in practice, recent works have proposed novel *complexity measures* for deep networks [Jiang et al., 2019, Keskar et al., 2016, Liang et al., 2017, Nagarajan and Kolter, 2019]. Such measures quantify the complexity of the function that a neural network represents. Ideally, such complexity measures should be good predictors of the degree of generalization of a network. However, in practice, such manually-designed complexity measures have failed to capture essential properties of generalization in deep networks such as improving with network size and worsening with label noise.

To overcome such limitations, we propose an alternative data-driven approach for constructing a complexity measure. Our model, Neural Complexity (NC), meta-learns a neural network that takes a predictor as input and outputs a scalar. Similarly to previous complexity-based generalization bounds, we provide a probabilistic bound of the true loss using NC. Our bound has very different characteristics from previous generalization bounds: it depends on both data distribution and architecture, and more importantly, becomes tighter as the NC model improves.

Experimentally, we show that a learned NC model consistently accelerates training in addition to preventing overfitting. We also show that the measure learned by NC can be transferred to different hypothesis classes such as using different network architecture, learning rate, or nonlinearity for the task learner. Compared to other recent meta-learning methods [Wu et al., 2018], the meta-learned knowledge in NC is much more stable across long learning trajectories. Finally, while most meta-learning works focus on improving performance on small tasks such as few-shot classification, we show that NC is also capable of regularizing learning in single large tasks.

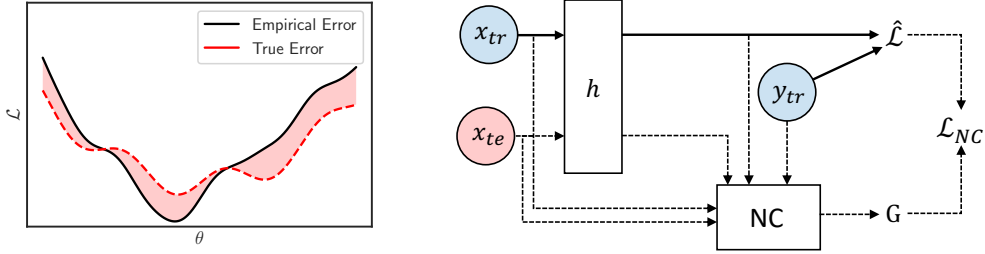


Figure 1: (left) The true and empirical losses are correlated but different. Neural Complexity (NC) estimates the difference between the two values (colored). (right) The standard training loss (solid lines) is regularized by the output of the trained NC model (dotted lines). NC is meta-learned so that \mathcal{L}_{NC} mimics the test loss.

2 Problem Setup

We adopt a meta-learning problem formulation where a model facilitates learning in new tasks by using previous experience learning in other related tasks. Specifically, we assume all tasks share sample space \mathcal{Z} , hypothesis space \mathcal{H} , and loss function $\mathcal{L} : \mathcal{H} \times \mathcal{Z} \rightarrow \mathbb{R}$. Each task T consists of i.i.d. sampled finite training set $S = \{z_1, \dots, z_m\}$ from the underlying hidden distribution D_T over the sample space \mathcal{Z} associated with task T . The *true loss* \mathcal{L}_T and *empirical loss* $\widehat{\mathcal{L}}_{T,S}$ for each task T are respectively defined as

$$\mathcal{L}_T(h) \stackrel{\text{def}}{=} \mathbb{E}_{z \sim D_T} [\mathcal{L}(h, z)] \quad \text{and} \quad \widehat{\mathcal{L}}_{T,S}(h) \stackrel{\text{def}}{=} \frac{1}{m} \sum_{z \in S} \mathcal{L}(h, z). \quad (1)$$

In the framework of meta-learning, tasks themselves are i.i.d. sampled from a task distribution: $T \sim \tau$. The objective of our meta-learner is to predict the *generalization gap* $G_{T,S}$, which is defined as the difference between the true and empirical losses:

$$G_{T,S}(h) = \mathcal{L}_T(h) - \widehat{\mathcal{L}}_{T,S}(h). \quad (2)$$

In other words, our model meta-learns a mapping $\mathcal{H} \rightarrow \mathbb{R}$ which mimics $h \mapsto G_{T,S}(h)$ by observing $\mathcal{L}_T(h)$ and $\widehat{\mathcal{L}}_{T,S}(h)$ in many different tasks that follow $T \sim \tau$.

Even with the practical setting where we only have a few or even a single task, we can still follow this problem formulation to meta-learn by constructing a set of tasks in the following way. Given one large dataset $S = \{z_1, \dots, z_M\}$, we randomly split S into disjoint training and validation sets. For each task with this random split, the task learner uses the train set to train h , and the meta-learner evaluates \mathcal{L}_T computed with the validation set as its target. After training a meta-learner on this simulated set of tasks, we use the same model to estimate the gap $G_{T,S}$ of the full dataset S .

3 Neural Complexity

We now describe Neural Complexity (NC), a neural network that directly meta-learns a complexity measure through interactions with many tasks. [Figure 1](#) shows the overall structure of NC, and [Figure 2](#) describes a more detailed diagram of its training loop. We also detail the training procedure of NC in [Algorithms 1](#) and [2](#).

3.1 Motivation: From Gap Estimate to Generalization Bound

We motivate our meta-learning objective through a simple method of extending the identity $\widehat{\mathcal{L}}_{T,S} + G_{T,S} = \mathcal{L}_T$ to a probabilistic bound of \mathcal{L}_T using any estimator of the gap $G_{T,S}$.

Proposition 1. *Let $D_{\mathcal{H}}$ be a distribution of hypotheses, and let $f : \mathcal{Z}^m \times \mathcal{H} \rightarrow \mathbb{R}$ be any function of the training set and hypothesis. Let D_{Δ} denote the distribution of $G_{T,S}(h) - f(S, h)$ where $h \sim D_{\mathcal{H}}$, and let $\Delta_1, \dots, \Delta_n$ follow D_{Δ} i.i.d.. The following holds for all $\epsilon > 0$:*

$$\mathbb{P} [\mathcal{L}_T(h) - \widehat{\mathcal{L}}_{T,S}(h) \leq f(S, h) + \epsilon] \geq 1 - \frac{|\{i | \Delta_i > \epsilon\}|}{n} - 2 \sqrt{\frac{\log \frac{2}{\delta}}{2n}}. \quad (3)$$

Algorithm 1 Task Learning with NC

Require: $X_{\text{tr}}, X_{\text{te}}, Y_{\text{tr}}, Y_{\text{te}}$

Randomly initialize parameters θ of learner h

loop

$\mathcal{L}_{\text{reg}} \leftarrow \widehat{\mathcal{L}}_{T,S}(h) + \lambda \cdot \text{NC}(X_{\text{tr}}, X_{\text{te}}, Y_{\text{tr}}, h(X_{\text{tr}}), h(X_{\text{te}}))$ NC-regularized task loss (4)

$\theta \leftarrow \theta - \nabla_{\theta} \mathcal{L}_{\text{reg}}$ Gradient step

end loop

$G_{T,S}(h) \leftarrow \mathcal{L}_T(h) - \widehat{\mathcal{L}}_{T,S}(h)$ Compute gap (2)

return Snapshot $H = (X_{\text{tr}}, X_{\text{te}}, Y_{\text{tr}}, h(X_{\text{tr}}), h(X_{\text{te}}), G_{T,S}(h))$

Algorithm 2 Meta-learning NC

Require: H_1, \dots, H_N Snapshots from different runs of [Algorithm 1](#)

Randomly initialize parameters ϕ of NC

while not converged **do**

Sample $H_i = (X_{\text{tr}}^i, X_{\text{te}}^i, Y_{\text{tr}}^i, h^i(X_{\text{tr}}^i), h^i(X_{\text{te}}^i), G_{T^i, S^i}(h^i))$ from H_1, \dots, H_N

$\Delta \leftarrow G_{T^i, S^i}(h^i) - \text{NC}(X_{\text{tr}}^i, X_{\text{te}}^i, Y_{\text{tr}}^i, h^i(X_{\text{tr}}^i), h^i(X_{\text{te}}^i))$

$\phi \leftarrow \phi - \nabla_{\phi} \mathcal{L}_{\text{NC}}(\Delta)$ NC's loss function (5)

end while

We defer the proof to the supplementary material. First note that the role of f in this bound mirrors that of complexity measures in previous generalization bounds. Since we can compute f given S and h , we can restate [Proposition 2](#) as stating that the regularized loss $\widehat{\mathcal{L}}_{T,S}(h) + f(S, h)$ differs from \mathcal{L}_T by at most ϵ (with the given probability). Furthermore, making f more accurately predict $G_{T,S}$ tightens this bound by decreasing the $\frac{|\{i|\Delta_i > \epsilon\}|}{n}$ term.

Taking motivation from this result, our NC meta-learns such a function f by regressing towards the gap $G_{T,S}$. This approach differs from traditional generalization bounds in the following ways. Rather than trying to design a measure of complexity that yields a tight generalization bound, we meta-learn such a measure in a data-driven way by posing the tightening of the bound as an optimization problem for the NC network to solve.

3.2 Training

We first illustrate NC's training loop. Recall from [Section 3](#) that we consider a meta-learning setup consisting of a set of related but different tasks. Given a task T with dataset S , the task learner runs SGD (or a variant of it) with respect to the following regularized loss:

$$\mathcal{L}_{\text{reg}}(h) = \widehat{\mathcal{L}}_{T,S}(h) + \lambda \cdot \text{NC}(S, h). \quad (4)$$

Note that the empirical loss $\widehat{\mathcal{L}}_{T,S}(h)$ is regularized by the output of NC. We set $\lambda = 0$ at initialization, and use a linear schedule where $\lambda = 1$ after a certain number of episodes.

The objective of NC is to estimate the difference between \mathcal{L}_T and $\widehat{\mathcal{L}}_{T,S}$ for any of the hypotheses h_0^T, \dots, h_N^T , for any task $T \sim \tau$. NC is a permutation-invariant neural network that takes a representation of the function h along with the training set as input and outputs a scalar. We train NC using the Huber loss [\[Huber, 1992\]](#) with target $G_{T,S}$:

$$\mathcal{L}_{\text{NC}}(\Delta) = \begin{cases} \frac{1}{2}\Delta^2 & \text{for } \Delta \leq 1 \\ |\Delta| - \frac{1}{2} & \text{otherwise} \end{cases}, \quad (5)$$

where $\Delta = G_{T,S}(h) - \text{NC}(h)$. We found that the Huber loss was more stable than the standard MSE loss, likely because the scale of $G_{T,S}$ can vary widely depending on h .

3.3 Architecture

We now describe the architecture of NC used in our experiments. We have mentioned in [Proposition 2](#) and [Equation 4](#) that NC takes a representation of the function h as input. We accomplish this by

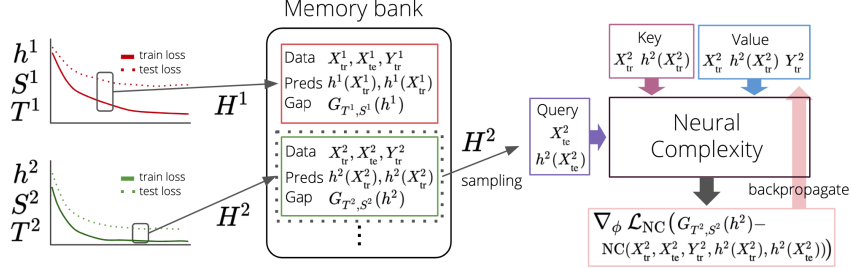


Figure 2: The *memory bank* stores snapshots from different training runs. During NC training, we uniformly sample mini-batches from the memory bank.

passing both data x and predictions $h(x)$ to NC. In terms of the function h , the tuple $(x, h(x))$ can be written as $\delta_x[(\text{id}, h)]$ where δ_x is the evaluation functional at x and id is the identity function. This representation of h captures the behavior of h at the datapoints considered during training and evaluation. In our experiments, this structure sufficed for extracting relevant features of h .

Regression We first describe NC when each task T is a regression task with vector data ($x \in \mathbb{R}^D$). Let $X_{\text{tr}} \in \mathbb{R}^{m \times D}$, $X_{\text{te}} \in \mathbb{R}^{m' \times D}$, $Y_{\text{tr}} \in \mathbb{R}^{m \times 1}$ denote train data, test data, and train labels, respectively. The learner’s hypothesis h produces outputs $h(X_{\text{tr}}) \in \mathbb{R}^{m \times 1}$ and $h(X_{\text{te}}) \in \mathbb{R}^{m' \times 1}$ for train and test data. NC first embeds all data with a shared encoding network f_{enc} , which is an MLP that operates row-wise on these matrices:

$$f_{\text{enc}}(X_{\text{tr}}) = e_{\text{tr}} \in \mathbb{R}^{m \times d}, \quad f_{\text{enc}}(X_{\text{te}}) = e_{\text{te}} \in \mathbb{R}^{m' \times d}. \quad (6)$$

These embeddings are fed into a multi-head attention layer [Vaswani et al., 2017] where queries, keys, and values are $Q = e_{\text{te}}$, $K = e_{\text{tr}}$, $V = [e_{\text{tr}}, y_{\text{tr}}] (\in \mathbb{R}^{m \times (d+1)})$, respectively. The output of this attention layer is a set of m' items, each corresponding to a test datapoint:

$$f_{\text{att}}(Q, K, V) = e_{\text{att}} \in \mathbb{R}^{m' \times d}. \quad (7)$$

Finally, these embeddings are passed through a decoding MLP network and averaged:

$$\text{NC}(X_{\text{tr}}, X_{\text{te}}, Y_{\text{tr}}, h(X_{\text{tr}}), h(X_{\text{te}})) = \frac{1}{m'} \sum_{i=1}^{m'} f_{\text{dec}}(e_{\text{att}})_i \in \mathbb{R}. \quad (8)$$

Note that NC is permutation invariant because it consists of permutation invariant components. This is important since NC’s objective is also invariant with respect to permutation of input datasets.

Classification The architecture of NC for classification tasks is identical to that of regression, except for the following additional interaction layer used to compute V . Representing labels as one-hot vectors in a classification task with c classes gives $Y_{\text{tr}} \in \mathbb{R}^{m' \times c}$. Instead of concatenating e_{tr} and Y_{tr} as in (14), we use a bilinear layer to produce V :

$$V = \mathbb{W}(e_{\text{tr}}, [Y_{\text{tr}}, \mathbf{1}, \mathcal{L}(X_{\text{tr}})]) \in \mathbb{R}^{m' \times d} \quad (\mathbb{W} \in \mathbb{R}^{d \times d \times (c+2)}). \quad (9)$$

Note that we concatenate a vector of ones and the train loss to Y_{tr} before passing into the bilinear layer; we perform an ablation study on each of these components in Section 5. This bilinear layer generalizes the interaction layer proposed in Xu et al. [2019]: while they explicitly choose a subnetwork to use according to class, (9) implicitly multiplies 0 to all but one of the c weights in each slice of the last dimension. Additionally, to scale NC up to high-dimensional image data such as the CIFAR dataset, we use a convolutional neural network for the encoder f_{enc} .

Because training runs (4) are time-consuming for large networks h , we use a *memory bank* to store and re-use the information necessary for the meta-learning loss (5). Specifically, we store tuples $(X_{\text{tr}}, X_{\text{te}}, Y_{\text{tr}}, h(X_{\text{tr}}), h(X_{\text{te}}))$ along with the observed gap $\hat{\mathcal{L}}_{T,S}(h) - \mathcal{L}_T(h)$. This memory bank has manageable memory cost because we can store only the indices for X_{tr} , X_{te} , and the other tensors have low dimensions. We randomly sample minibatches of such tuples to train NC with the meta-learning loss (5). Figure 2 shows how the memory bank interacts with NC.

3.4 Interpretations

We provide several interpretations of estimating the generalization gap $G_{T,S}$ using a neural network.

Meta-learned Complexity Measure As mentioned in Section 1, many recent works attempt to understand generalization in deep networks by proposing novel complexity measures. Such measures are designed to correlate well with generalization while being directly computable for any given set of parameters. NC can be seen as a meta-learned complexity measure, and its target (2) is the generalization gap. Instead of hand-designing an appropriate complexity measure, NC meta-learns it by regressing towards observed degrees of generalization.

Optimal Regularizer A standard approach to generalization is to augment the empirical loss $\hat{\mathcal{L}}_{T,S}$ by adding a regularization term λ : $\mathcal{L}_{\text{reg}} = \hat{\mathcal{L}}_{T,S}(h) + \lambda(h)$. Since the purpose of λ is to make the regularized loss \mathcal{L}_{reg} close to the true loss \mathcal{L}_T , we argue that the *optimal regularizer* for task T is the function that makes $\mathcal{L}_{\text{reg}}(h) = \mathcal{L}_T(h)$ for all h . This unique "optimal regularizer" is exactly $G_{T,S}$; therefore, NC can be seen as a meta-learned regularizer for which the target is the optimal regularizer.

A Smaller Sufficient Statistic of True Loss We contrast the graphical models of NC with the Neural Process (NP) [Garnelo et al., 2018] in Figure 3. Both approaches involve a single meta-learner which observes multiple tasks with the goal of achieving low test loss. The two approaches infer different sufficient statistics for the true loss \mathcal{L}_T . NP infers the data distribution of T and NC infers the gap G . While both G and the data distribution are sufficient for reconstructing \mathcal{L}_T , G has much lower dimension: $G(h) \in \mathbb{R}$, whereas T is a distribution over $\mathcal{X} \times \mathcal{Y} = \mathbb{R}^{d_X+d_Y}$.

Actor-Critic Generalizing to unseen test data can be seen as a reinforcement learning environment with known dynamics: train data and train loss is observed, and the selection of each hypothesis h is an action. The objective is to maximize the return, which is the negative true loss ($-\mathcal{L}_T$). Our approach can be seen as an actor-critic method where NC is the learned value function.

4 Related Works

Complexity Measures for Deep Networks The question of why deep networks generalize despite being over-parameterized has been the focus of many recent works. Building on traditional generalization theory [Vapnik, 1999, McAllester, 1999], such works have adapted PAC-Bayes bounds [Dziugaite and Roy, 2017, Zhou et al., 2018] and norm-based bounds [Neyshabur et al., 2015, Bartlett et al., 2017] to deep networks. Other works have proposed measures that empirically correlate with generalization [Keskar et al., 2016, Liang et al., 2017, Nagarajan and Kolter, 2019]. This work proposes an alternative approach to the problem of explaining generalization. While these previous works rely on human-designed measures of complexity, we instead meta-learn such a measure. Because it is learned end-to-end rather than designed, our measure is able to take into account the distribution of tasks and the specific train dataset of a given task.

Meta-Learning Our method falls within the framework of meta-learning [Thrun and Pratt, 1998, Schmidhuber et al., 1996], in which a model learns useful information about the learning process itself through interactions with a set of different but related tasks. Recent methods formulate the meta-learning problem as learning optimizers [Ravi and Larochelle, 2016], data embeddings [Snell et al., 2017], initial parameters [Finn et al., 2017], or parameter priors [Kim et al., 2018]. A key difference is that NC is learner-agnostic: we can use an NC model trained on one class of task learners to regularize other task learners (e.g. different architecture, activation, optimizer). Additionally, using NC's output as a regularization loss makes it more stable in long training runs compared to previous meta-learning algorithms.

MetaReg [Balaji et al., 2018], which proposes to learn a weighted L_1 regularization loss, is probably the most similar work to ours since they also learn a regularizer in a meta-learning setup. However,

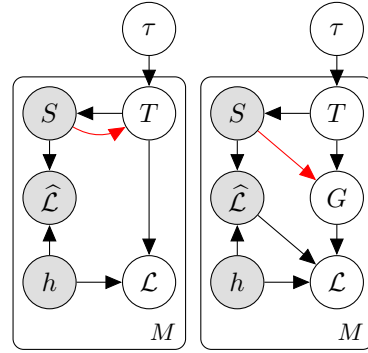


Figure 3: Graphical models corresponding to (left) Neural Processes and (right) NC. Observed nodes are shaded and red arrows denote amortized inference.

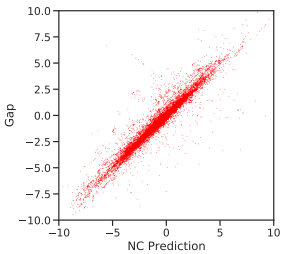


Figure 4: NC predictions and true gap values.

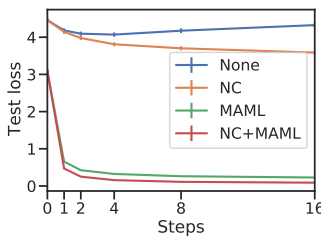


Figure 5: Test loss of combinations of NC and MAML.

their regularizer cannot be used on different network architectures because it operates in parameter space. Furthermore, even on the same architecture, their method requires reusing the feature network for the learned L_1 loss weights to be meaningful. In contrast, NC learns a complexity measure in function space, allowing it to generalize to different architectures and to completely initialized networks.

5 Experiments

5.1 Sinusoid Regression

To illustrate the basic properties of NC, we begin with a toy sinusoid regression problem introduced in Finn et al. [2017]. Each task is a sine function $x \mapsto A \sin(x + b)$ where x, A, b are uniformly sampled from $[-5, 5], [0.1, 5]$ and $[0, \pi]$, respectively. We consider 10-shot learning and use the mean squared error as the loss function. During meta-training, the layer size, activation, number of layers, learning rate, and number of steps were all fixed to $(40, \text{ReLU}, 2, 0.01, 16)$, respectively.

NC-Gap Fit In Figure 4, we compare the predictions of a trained NC model with the generalization gap $G_{T,S}$ for many batches. These two values are strongly correlated ($R^2 = 0.9589$), indicating that NC is indeed capable of predicting the gap based on the complexity of the learner’s hypothesis h .

VS Other Regularizers We compared NC against various other regularization methods. We report these results in the appendix due to space issues. NC performs all other methods by a large margin because learners tend to overfit very quickly in this few-shot regression problem.

Integration with MAML We investigated whether NC can integrate with MAML [Finn et al., 2017], an alternative meta-learning approach. We first trained a MAML model and then trained NC using snapshots obtained from MAML trajectories. Figure 5 shows that NC successfully reduces the final test loss for both settings: with and without MAML initializations. These results indicate that the regularization effect of NC is orthogonal to that of MAML, and that future improvements in either direction can benefit the other.

Learning Curve We show the train and test loss curves of a task learner regularized by NC in Figure 7. The test loss is lower than the train loss throughout training, which is a trend that we observed in all experimental settings we considered. In other words, the estimate of NC is a precise enough surrogate for $G_{T,S}$ that minimizing it results in negative $G_{T,S}$.

5.2 Out-of-distribution Task Learners

Visualization of Simple Learners We observed the behavior of NC when given hypotheses from closed-form learners with very distinct properties. We consider a constant learner which simply returns the average of all y in the train set along with a nearest neighbor learner. We show $(X_{\text{tr}}, X_{\text{te}}, Y_{\text{tr}}, Y_{\text{te}}, h(X_{\text{tr}}), h(X_{\text{te}}))$ and gap values along with NC predictions in Figure 8. Note that while we show test targets Y_{te} in the figure, NC does not observe them. While both functions h do not follow the shape of a typical sine function, NC only penalizes the function on the right since it perfectly fits only the train set.

Changing NN Learner Hyperparameters We evaluated how well NC can generalize to other task learners on the sinusoid regression task in Section 5.1. We measured performance while alternating

Method	Accuracy
Full	92.93
- Huber loss	89.74
- Bias	84.30
- Loss conditioning	72.09
- Bilinear layer	23.69

Figure 6: Ablation study; we sequentially removed each architectural component.

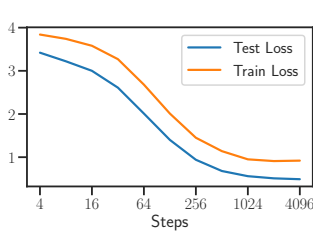


Figure 7: Train and test loss curves of NC regularization.

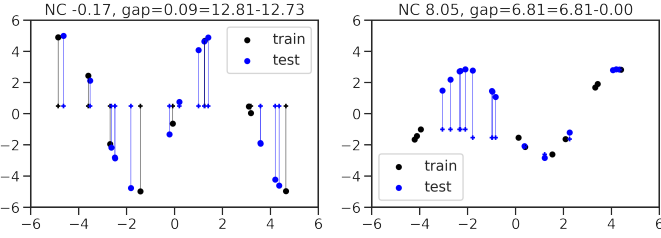


Figure 8: Visualization of regression tasks using different learners: (left) a constant function and (right) nearest neighbors. Circles and plus signs represent targets and predictions.

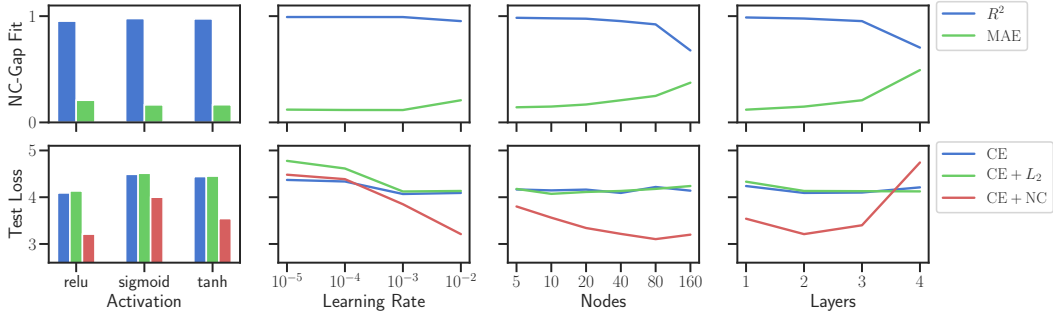


Figure 9: Evaluation of Out-of-distribution task learners. The x axis shows the altered learner hyperparameter. (top) NC-gap fit statistics and (bottom) test loss after learning with NC and baselines.

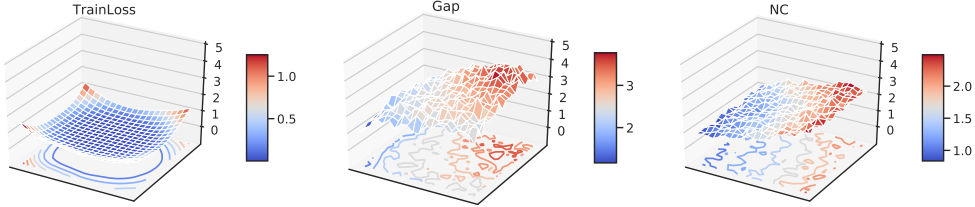


Figure 10: Visualization of loss surfaces. Best viewed zoomed in.

four different learning algorithm hyperparameters: activation, learning rate, nodes per layer, and the number of layers. We used the same NC model which was trained using only (relu, 10^{-2} , 40, 2) for these hyperparameters. In Figure 9, we measure how well NC fits the $G_{T,S}$ through their R^2 statistic and their mean absolute error (MAE). NC’s predictions are accurate even when the learners are changed, only degrading when the learner is significantly more expressive (160 nodes and 4 layers). Figure 9 additionally reports the test losses of NC regularization compared to the cross-entropy loss and L_2 regularization. NC regularization shows consistent improvements except for when the network architecture was too different (4 layers). This experiment demonstrates that NC’s complexity measure captures the properties of h itself, regardless of its specific parameterization. We emphasize that such a transfer between different task learners is not possible with other meta-learning approaches. [Finn et al., 2017, Snell et al., 2017, Garnelo et al., 2018].

5.3 Few-shot Image Classification

Ablation Study To validate our architectural choices for NC, we performed an ablation experiment using a 10-way 1-shot classification task on the Omniglot Lake et al. [2015] dataset. Results in Figure 6 show the performance of several architectures for NC. First note that removing Huber loss and using MSE loss degrades performance, likely due to large gradients when the difference between NC’s prediction and $G_{T,S}$ is large. Furthermore, removing any of the additional components for the classification model (bias, train loss, bilinear layer) reduces accuracy, with the bilinear layer being the most critical for performance.

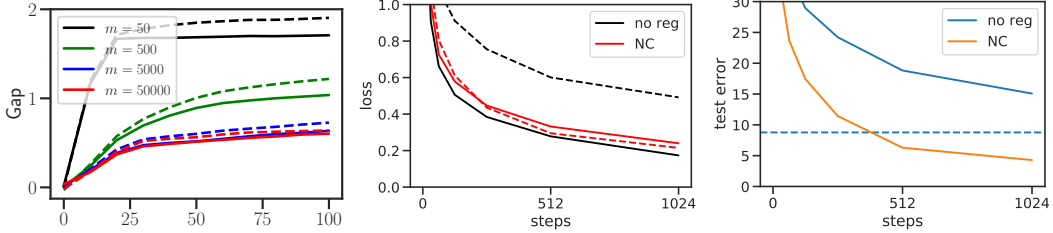


Figure 11: Single-task regularization on the KMNIST dataset. Left: NC estimates (solid lines) and gap values (dashed lines) when training with datasets of different size. Center: Learning curve of train (solid lines) and test (dashed lines) losses with and without NC. Right: Learning curve of test error with and without NC. The dashed horizontal line represents baseline performance after convergence.

	MNIST	FMNIST	KMNIST	SVHN	CIFAR-10
Cross-Entropy	98.31 ± 0.12	88.21 ± 0.05	91.12 ± 0.08	93.23 ± 0.44	79.76 ± 0.34
L_2 Regularization	98.36 ± 0.06	88.46 ± 0.17	91.31 ± 0.05	94.06 ± 0.44	79.84 ± 0.75
Label Smoothing Szegedy et al. [2016]	98.57 ± 0.11	89.15 ± 0.40	91.40 ± 0.05	94.70 ± 0.38	80.45 ± 0.44
Mixup Zhang et al. [2017]	97.80 ± 0.27	89.50 ± 0.16	91.10 ± 0.17	94.88 ± 0.24	80.92 ± 0.47
NC Regularization	99.03 ± 0.07	89.74 ± 0.17	96.30 ± 0.07	93.83 ± 0.18	81.15 ± 0.36

Table 1: Mean test accuracies and 95% confidence intervals of each method on 5 runs.

Loss Surface Visualization We use the filter-wise normalization technique introduced in [Li et al. \[2018\]](#) to visualize the loss surfaces of a learner at convergence. [Figure 10](#) shows that the train loss is at a stable local minimum, but the generalization gap can decrease further by moving in a specific direction. Because NC correctly captures the trend of the gap, minimizing the NC-regularized loss would move the learner to a region with lower test loss.

5.4 Single Image Classification Tasks

Finally, we evaluate NC on single tasks, following our protocol outlined in [Section 3](#) of constructing a large number of sub-tasks using only the train split and then evaluating on the test set. We consider five different datasets: three MNIST variants (MNIST [LeCun \[1998\]](#), FMNIST [Xiao et al. \[2017\]](#), KMNIST [Clanuwat et al. \[2018\]](#)), for which the learner was a 1-layer MLP with 500 units, and SVHN [Netzer et al. \[2011\]](#) along with CIFAR-10 [Krizhevsky et al. \[2009\]](#), for which we used the ResNet-18 [He et al. \[2016\]](#) network. To isolate the effect of the regularizers, we do not use image augmentation or manual learning rate scheduling. Due to space constraints, we describe detailed hyperparameters and NC architectures in the appendix.

Effect of Dataset Size We investigated whether NC can capture the effect of dataset size m on overfitting. Using an unregularized learner on the KMNIST dataset, we measured how the gap and NC’s estimate of it changes during task learning. The left figure of [Figure 11](#) shows that overfitting occurs more severely with smaller datasets, and NC successfully captures this trend.

Regularization Performance We measure NC’s effectiveness as a regularizer, comparing it to other regularization methods for classification tasks. We consider four baselines: standard cross-entropy loss, L_2 loss, label smoothing [Szegedy et al. \[2016\]](#), and mixup [Zhang et al. \[2017\]](#). Results in [Table 1](#) show that NC consistently improves test accuracy and performs similarly to modern regularization methods, even outperforming them on some tasks. We further visualize the learning curve of a NC-regularized task learner on the KMNIST dataset in the middle and right figures of [Figure 11](#), which show that NC accelerates training in addition to improving the final accuracy.

6 Conclusion

We introduced Neural Complexity (NC), a model that learns the degree to which a function will generalize to unseen test data. Unlike previous meta-learning models, NC can regularize task learners

from previously unseen hypothesis classes. Additionally, our experiments demonstrate that NC can learn to regularize single large tasks by sampling multiple tasks from the train set. We see many exciting future directions for NC such as scaling it up to the ImageNet dataset [Deng et al. \[2009\]](#) or applying it to predicting the generalization gap in unsupervised learning problems such as density estimation.

Broader Impact

Safety and reliability are important desiderata for machine learning models, and these properties are even more important given the recent success of black-box models such as deep neural networks. Our proposed approach can be applied to improve training in any regression or classification task, and our experiments demonstrate its ability to (1) predict the generalization gap and (2) improve test loss when used as a regularizer. NC’s data-driven prediction of the generalization gap can serve as an approximate guarantee for safety-critical problems. Furthermore, future extensions of NC may enable previously impossible tasks since NC was particularly effective in settings where conventional learners overfitted.

References

Y. Balaji, S. Sankaranarayanan, and R. Chellappa. Metareg: Towards domain generalization using meta-regularization. In *Advances in Neural Information Processing Systems*, pages 998–1008, 2018.

P. L. Bartlett, D. J. Foster, and M. J. Telgarsky. Spectrally-normalized margin bounds for neural networks. In *Advances in Neural Information Processing Systems*, pages 6240–6249, 2017.

T. Clanuwat, M. Bober-Irizar, A. Kitamoto, A. Lamb, K. Yamamoto, and D. Ha. Deep learning for classical Japanese literature, 2018.

J. Deng, W. Dong, R. Socher, L.-J. Li, K. Li, and L. Fei-Fei. Imagenet: A large-scale hierarchical image database. In *2009 IEEE conference on computer vision and pattern recognition*, pages 248–255. Ieee, 2009.

A. Dvoretzky, J. Kiefer, and J. Wolfowitz. Asymptotic minimax character of the sample distribution function and of the classical multinomial estimator. *The Annals of Mathematical Statistics*, pages 642–669, 1956.

G. K. Dziugaite and D. M. Roy. Computing nonvacuous generalization bounds for deep (stochastic) neural networks with many more parameters than training data. *arXiv preprint arXiv:1703.11008*, 2017.

C. Finn, P. Abbeel, and S. Levine. Model-agnostic meta-learning for fast adaptation of deep networks. *arXiv preprint arXiv:1703.03400*, 2017.

M. Garnelo, J. Schwarz, D. Rosenbaum, F. Viola, D. J. Rezende, S. Eslami, and Y. W. Teh. Neural processes. *arXiv preprint arXiv:1807.01622*, 2018.

K. He, X. Zhang, S. Ren, and J. Sun. Deep residual learning for image recognition. In *Proceedings of the IEEE conference on computer vision and pattern recognition*, pages 770–778, 2016.

P. J. Huber. Robust estimation of a location parameter. In *Breakthroughs in statistics*, pages 492–518. Springer, 1992.

Y. Jiang, B. Neyshabur, H. Mobahi, D. Krishnan, and S. Bengio. Fantastic generalization measures and where to find them. *arXiv preprint arXiv:1912.02178*, 2019.

N. S. Keskar, D. Mudigere, J. Nocedal, M. Smelyanskiy, and P. T. P. Tang. On large-batch training for deep learning: Generalization gap and sharp minima. *arXiv preprint arXiv:1609.04836*, 2016.

T. Kim, J. Yoon, O. Dia, S. Kim, Y. Bengio, and S. Ahn. Bayesian model-agnostic meta-learning. *arXiv preprint arXiv:1806.03836*, 2018.

M. R. Kosorok. *Introduction to empirical processes and semiparametric inference*. Springer Science & Business Media, 2007.

A. Krizhevsky, G. Hinton, et al. Learning multiple layers of features from tiny images. 2009.

A. Krizhevsky, I. Sutskever, and G. E. Hinton. Imagenet classification with deep convolutional neural networks. In *Advances in neural information processing systems*, pages 1097–1105, 2012.

B. M. Lake, R. Salakhutdinov, and J. B. Tenenbaum. Human-level concept learning through probabilistic program induction. *Science*, 350(6266):1332–1338, 2015.

Y. LeCun. The mnist database of handwritten digits. <http://yann.lecun.com/exdb/mnist/>, 1998.

Y. Lee and S. Choi. Gradient-based meta-learning with learned layerwise metric and subspace. 2018.

H. Li, Z. Xu, G. Taylor, C. Studer, and T. Goldstein. Visualizing the loss landscape of neural nets. In *Advances in Neural Information Processing Systems*, pages 6389–6399, 2018.

T. Liang, T. Poggio, A. Rakhlin, and J. Stokes. Fisher-rao metric, geometry, and complexity of neural networks. *arXiv preprint arXiv:1711.01530*, 2017.

P. Massart. The tight constant in the dvoretzky-kiefer-wolfowitz inequality. *The annals of Probability*, pages 1269–1283, 1990.

D. A. McAllester. Pac-bayesian model averaging. In *COLT*, volume 99, pages 164–170. Citeseer, 1999.

V. Nagarajan and J. Z. Kolter. Generalization in deep networks: The role of distance from initialization. *CoRR*, abs/1901.01672, 2019. URL <http://arxiv.org/abs/1901.01672>.

Y. Netzer, T. Wang, A. Coates, A. Bissacco, B. Wu, and A. Y. Ng. Reading digits in natural images with unsupervised feature learning. 2011.

B. Neyshabur, R. Tomioka, and N. Srebro. Norm-based capacity control in neural networks. In *Conference on Learning Theory*, pages 1376–1401, 2015.

S. Ravi and H. Larochelle. Optimization as a model for few-shot learning. 2016.

J. Schmidhuber, J. Zhao, and M. Wiering. Simple principles of metalearning. *Technical report IDSIA*, 69:1–23, 1996.

D. Silver, T. Hubert, J. Schrittwieser, I. Antonoglou, M. Lai, A. Guez, M. Lanctot, L. Sifre, D. Kumaran, T. Graepel, et al. Mastering chess and shogi by self-play with a general reinforcement learning algorithm. *arXiv preprint arXiv:1712.01815*, 2017.

J. Snell, K. Swersky, and R. Zemel. Prototypical networks for few-shot learning. In *Advances in Neural Information Processing Systems*, pages 4077–4087, 2017.

N. Srivastava, G. Hinton, A. Krizhevsky, I. Sutskever, and R. Salakhutdinov. Dropout: a simple way to prevent neural networks from overfitting. *The journal of machine learning research*, 15(1):1929–1958, 2014.

C. Szegedy, V. Vanhoucke, S. Ioffe, J. Shlens, and Z. Wojna. Rethinking the inception architecture for computer vision. In *Proceedings of the IEEE conference on computer vision and pattern recognition*, pages 2818–2826, 2016.

S. Thrun and L. Pratt. Learning to learn: Introduction and overview. In *Learning to learn*, pages 3–17. Springer, 1998.

V. N. Vapnik. An overview of statistical learning theory. *IEEE transactions on neural networks*, 10(5):988–999, 1999.

A. Vaswani, N. Shazeer, N. Parmar, J. Uszkoreit, L. Jones, A. N. Gomez, Ł. Kaiser, and I. Polosukhin. Attention is all you need. In *Advances in neural information processing systems*, pages 5998–6008, 2017.

Y. Wu, M. Ren, R. Liao, and R. Grosse. Understanding short-horizon bias in stochastic meta-optimization. *arXiv preprint arXiv:1803.02021*, 2018.

H. Xiao, K. Rasul, and R. Vollgraf. Fashion-mnist: a novel image dataset for benchmarking machine learning algorithms. *arXiv preprint arXiv:1708.07747*, 2017.

J. Xu, J.-F. Ton, H. Kim, A. R. Kosiorek, and Y. W. Teh. Metafun: Meta-learning with iterative functional updates. *arXiv preprint arXiv:1912.02738*, 2019.

H. Zhang, M. Cisse, Y. N. Dauphin, and D. Lopez-Paz. mixup: Beyond empirical risk minimization. *arXiv preprint arXiv:1710.09412*, 2017.

W. Zhou, V. Veitch, M. Austern, R. P. Adams, and P. Orbanz. Non-vacuous generalization bounds at the imagenet scale: a pac-bayesian compression approach. *arXiv preprint arXiv:1804.05862*, 2018.

A Proof of Motivating Bound

We first invoke the following lemma, which relates the empirical and true cumulative distribution functions of i.i.d. random variables.

Lemma 1 (Dvoretzky–Kiefer–Wolfowitz Inequality). *Let X_1, \dots, X_n be i.i.d. random variables with cumulative distribution function (CDF) $F(\cdot)$. Denote the associated empirical CDF as $F_n(x) \triangleq \frac{1}{n} \sum_{i=1}^n \mathbf{1}_{\{X_i \leq x\}}$. The following inequality holds for all x w.p. $\geq 1 - \delta$:*

$$|F_n(x) - F(x)| \leq \sqrt{\frac{\log \frac{2}{\delta}}{2n}}. \quad (10)$$

Proof. We omit the proof. The original theorem appears in [Dvoretzky et al. \[1956\]](#) and was refined by [Massart \[1990\]](#). This two-sided version appears in [Kosorok \[2007\]](#). \square

Proposition 2. *Let $D_{\mathcal{H}}$ be a distribution of hypotheses, and let $f : \mathcal{Z}^m \times \mathcal{H} \rightarrow \mathbb{R}$ be any function of the training set and hypothesis. Let D_{Δ} denote the distribution of $G_{T,S}(h) - f(S, h)$ where $h \sim D_{\mathcal{H}}$, and let $\Delta_1, \dots, \Delta_n$ follow D_{Δ} i.i.d.. The following holds for all $\epsilon > 0$:*

$$\mathbb{P} \left[\mathcal{L}_T(h) - \widehat{\mathcal{L}}_{T,S}(h) \leq f(S, h) + \epsilon \right] \geq 1 - \frac{|\{i | \Delta_i > \epsilon\}|}{n} - 2\sqrt{\frac{\log \frac{2}{\delta}}{2n}}. \quad (11)$$

Proof. Let $F(x), F_n(x)$ be the CDF and empirical CDF of Δ , respectively.

$$\mathbb{P} \left(|\widehat{\mathcal{L}}_{T,S}(h) + \text{NC}_S(h) - \mathcal{L}_T(h)| > \epsilon \right) = \mathbb{P}_{\Delta \sim p_{NC}} (|\Delta| > \epsilon) = F(\epsilon) - F(-\epsilon). \quad (12)$$

By [Lemma 1](#), the following holds with probability $\geq 1 - \delta$:

$$F(\epsilon) - F(-\epsilon) \leq F_n(\epsilon) - F_n(-\epsilon) + 2\sqrt{\frac{\log \frac{2}{\delta}}{2n}} = \frac{n_{\epsilon}}{n} + 2\sqrt{\frac{\log \frac{2}{\delta}}{2n}}. \quad (13)$$

\square

B Additional Experiments

We evaluated the performance of the following regularizers on the sinusoid regression task: L_1 norm, L_2 norm, $L_{1,\infty}$ norm, $L_{3,1.5}$ norm, Orthogonal constraint, Frobenius norm, Dropout [[Srivastava et al., 2014](#)], MetaReg [[Balaji et al., 2018](#)], and NC. We show performance after $\{1, 2, 4, 8, 16\}$ steps. Results in [Table 2](#) show that all other baselines fail to provide guidance in this task, while NC outperforms them by a large margin.

In [Figure 12](#), we show additional visualizations of regression tasks. This figure shows that NC successfully captures the trend of the generalization gap even in out-of-distribution hypothesis classes.

[Figure 13](#) shows additional visualizations of loss surfaces, and reveals that the NC-regularized loss has similar trends to that of the test loss.

C Experimental Details

All experiments were ran on single GPUs (either Titan V or Titan XP) with the exception of the single-task image classification experiment, which was run on two.

These embeddings are fed into a multi-head attention layer [[Vaswani et al., 2017](#)] where queries, keys, and values are $Q = e_{\text{te}}, K = e_{\text{tr}}, V = [e_{\text{tr}}, y_{\text{tr}}] (\in \mathbb{R}^{m \times (d+1)})$, respectively. The output of this attention layer is a set of m' items, each corresponding to a test datapoint:

$$f_{\text{att}}(Q, K, V) = e_{\text{att}} \in \mathbb{R}^{m' \times d}. \quad (14)$$

Finally, these embeddings are passed through a decoding MLP network and averaged:

$$\text{NC}(X_{\text{tr}}, X_{\text{te}}, Y_{\text{tr}}, h(X_{\text{tr}}), h(X_{\text{te}})) = \frac{1}{m'} \sum_{i=1}^{m'} f_{\text{dec}}(e_{\text{att}})_i \in \mathbb{R}. \quad (15)$$

Steps	1	2	4	8	16
No regularization	4.17	4.04	4.05	4.04	4.05
$L_1(\lambda = 10.0)$	4.21	4.26	4.26	4.25	4.25
$L_1(\lambda = 1.0)$	4.08	4.00	3.98	4.03	4.13
$L_1(\lambda = 0.1)$	4.07	3.98	3.95	4.01	4.12
$L_1(\lambda = 0.01)$	4.08	3.98	3.95	4.04	4.16
$L_2(\lambda = 10.0)$	4.10	4.11	4.17	4.22	4.32
$L_2(\lambda = 1.0)$	4.08	3.98	3.94	3.96	4.00
$L_2(\lambda = 0.1)$	4.07	3.98	4.03	4.03	4.14
$L_2(\lambda = 0.01)$	4.08	3.98	3.96	4.04	4.16
$L_{1,\infty}(\lambda = 1.0)$	4.08	4.04	4.07	4.08	4.08
$L_{1,\infty}(\lambda = 0.1)$	4.07	3.98	3.95	4.01	4.12
$L_{1,\infty}(\lambda = 0.01)$	4.08	3.98	3.96	4.04	4.16
$L_{3,1.5}(\lambda = 1.0)$	4.07	4.03	4.11	4.09	4.07
$L_{3,1.5}(\lambda = 0.1)$	4.08	3.99	3.95	4.00	4.08
$L_{3,1.5}(\lambda = 0.01)$	4.07	3.98	3.95	4.04	4.15
Orthogonal ($\lambda = 1.0$)	4.16	4.17	4.19	4.22	4.32
Orthogonal ($\lambda = 0.1$)	4.08	4.00	3.96	3.99	4.06
Orthogonal ($\lambda = 0.01$)	4.07	3.98	3.95	4.03	4.14
Frobenius ($\lambda = 1.0$)	4.08	4.01	4.04	4.13	4.13
Frobenius ($\lambda = 0.1$)	4.07	3.98	3.95	4.02	4.11
Frobenius ($\lambda = 0.01$)	4.08	3.98	3.96	4.04	4.15
Dropout ($p = 0.1$)	4.08	3.98	3.96	4.04	4.15
Dropout ($p = 0.3$)	4.08	3.98	3.95	4.02	4.12
Dropout ($p = 0.5$)	4.08	3.99	3.95	4.00	4.07
Dropout ($p = 0.7$)	4.10	4.00	3.96	3.98	4.02
Dropout ($p = 0.9$)	4.17	4.11	4.09	4.37	NaN
MetaReg	4.04	3.93	3.89	3.90	4.00
Neural Complexity	3.87	3.60	3.36	3.13	2.93

Table 2: Test losses of various regularization methods after a certain number of steps.

C.1 Sinusoid Regression

Task Learner The learner was a one-layer MLP network with 40 hidden units and ReLU activations, and was trained with vanilla SGD with a learning rate of 0.01.

NC Architecture Datapoints x are encoded using an MLP encoder with n_{enc} layers, d -dimensional activations, and ReLU nonlinearities. The outputs of the encoder are fed into a multi-head attention layer with d -dimensional activations. The outputs of the multi-head attention layer are mean-pooled and fed into an MLP decoder with n_{dec} layers, d -dimensional activations, and ReLU nonlinearities. We train NC with batch size bs and the Adam optimizer with learning rate lr .

We considered the following range of hyperparameters: $n_{\text{enc}} \in \{1, 2, 3\}$, $d \in \{128, 256, 512, 1024\}$, $n_{\text{dec}} \in \{1, 2, 3\}$, $\text{bs} \in \{128, 256, 512, 1024\}$, $\text{lr} \in \{0.005, 0.001, 0.0005, 0.0001\}$. We tuned these hyperparameters with a random search and ultimately used $n_{\text{enc}} = 3$ $d = 1024$ $n_{\text{dec}} = 3$ $\text{bs} = 512$ $\text{lr} = 0.0005$.

C.2 Classification

Task Learner The task learner was ResNet-18 [He et al., 2016] for the SVHN and CIFAR-10 datasets, and an MLP with one hidden layer of 500 nodes and ReLU nonlinearities. To isolate the effect of the regularizers, we considered no data augmentation besides whitening. We train all networks with SGD with a fixed learning rate and no additional learning rate scheduling. The learning rate was 0.0001 for ResNet-18 and 0.01 for the MLP.

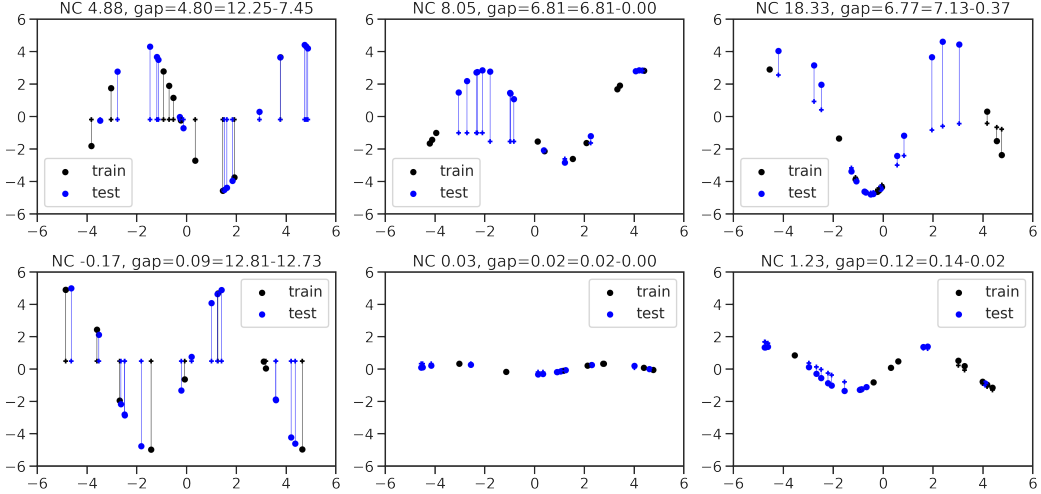


Figure 12: Visualization of regression tasks. The x and y axes represent inputs and outputs of the task learners, respectively. Circles represent the targets and plus signs represent predictions. The NC model is trained with a neural network learner, and we evaluated on three different learners: 0-th order polynomial (left), nearest-neighbor (center), and neural networks (right).

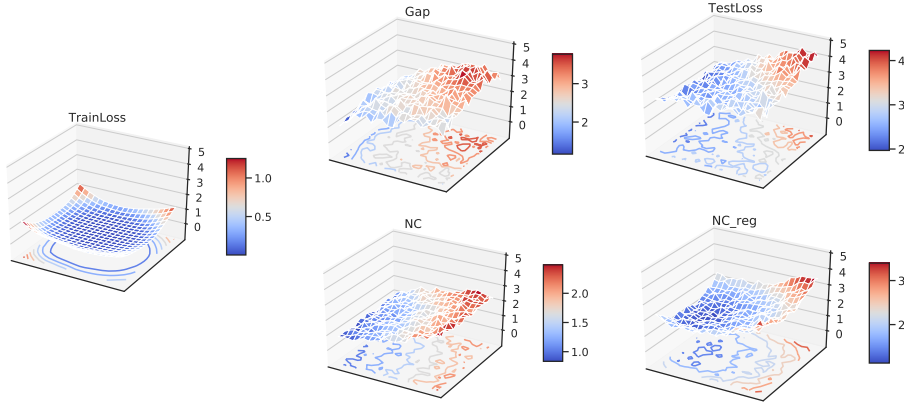


Figure 13: Visualization of loss surfaces. Best viewed zoomed in.

NC Architecture Datapoints x are encoded using a shared CNN encoder. The CNN architecture was the 4-layer convolutional net in [Snell et al., 2017] when the task learner was an MLP, and was ResNet-18 otherwise. We freeze all batch normalization layers inside NC. The outputs for only the train data is fed into a n_{enc} -layer MLP followed by a stack of n_{self} self-attention layers, both with d -dimensional activations. These outputs are processed by a bilinear layer, and all outputs are fed into a multi-head attention layer with d -dimensional activations. The outputs of the multi-head attention layer are then fed into an MLP decoder with n_{dec} layers, d -dimensional activations, and ReLU nonlinearities. We train NC with batch size bs and the Adam optimizer with learning rate lr .

For the MLP learners, we considered the following range of hyperparameters: $n_{enc} \in \{1, 2, 3\}$, $n_{self} \in \{1, 2, 3\}$, $d \in \{60, 120, 240\}$, $n_{dec} \in \{1, 2, 3\}$, $bs \in \{4, 8, 16\}$, $lr \in \{0.0005\}$. We tuned these hyperparameters with a random search and ultimately used $n_{enc} = 1$, $n_{self} = 1$, $d = 120$, $n_{dec} = 3$, $bs = 16$, $lr = 0.0005$.

For the ResNet-18 learners, we considered the following range of hyperparameters: $n_{enc} \in \{1, 2, 3\}$, $n_{self} \in \{1, 2, 3\}$, $d \in \{200, 400, 800, 1600\}$, $n_{dec} \in \{1, 2, 3\}$, $bs \in \{2, 4, 8\}$, $lr \in \{0.0005\}$. We tuned these hyperparameters with a random search and ultimately used $n_{enc} = 1$, $n_{self} = 3$, $d = 400$, $n_{dec} = 3$, $bs = 4$, $lr = 0.0005$.

Single-task Experiment Details We provide further details about the single-task experiments. The datasets we considered had either 50000 or 60000 training datapoints. We constructed learning tasks from such training sets by sampling 40000 "training" datapoints and 10000 validation datapoints. Using such splits, we trained NC as usual. To scale to long learning trajectories, we trained NC using one process, while simultaneously adding trajectories from a separate process on a separate GPU which only ran task learners regularized by the NC model. During final evaluation, we clipped NC estimates below -0.1 , which has the effect of ignoring NC when it is overconfident about generalization. We found that such clipping is critical for performance on long training runs.